Spring 5-8-2011

Modeling Human Immune Response to the Lyme Disease-Causing Bacteria

Yevhen Rutovytskyy

University of Connecticut - Storrs, rutovytskyy@yahoo.com

Modeling Human Immune Response to the Lyme Disease-Causing Bacteria

Yevhen Rutovytskyy (Peoplesoft ID 1593993)

5/13/2011

Honors Thesis Advisors:

Dr. Charles Wolgemuth

(Department of Molecular and Cell Biology at the University of Connecticut)

Dr. Greg Huber

(Department of Mathematics, Department of Molecular and Cell Biology at the University of Connecticut)

Contents

Abstract

The purpose of this project is to develop and analyze a mathematical model for the pathogen-host interaction that occurs during early Lyme disease (i.e., the initiation and spread of the Erythema Migrants rash). Based on the known biophysics of motility of *Borrelia burgdorferi* and a simple model for the immune response, a PDE model was created which tracks the time evolution of the concentrations of bacteria and activated immune cells in the dermis. We assume that a tick bite inoculates a highly localized population of bacteria into the dermis. These bacteria can multiply and migrate. The diffusive nature of the migration is assumed and modeled using the heat equation. Bacteria in the skin locally activate immune cells, such as macrophages. These cells track down the bacteria and kill them.

The immune cells' "tracking" of the bacteria is modeled using the Keller-Segel model for chemotaxis. Additionally, we assume that the rate that the immune cells consume the bacteria is proportional to the product of the concentrations of the bacteria and the immune cells.

Assuming the periodic boundary condition, the model is investigated over a 1D Cartesian domain. Once the equations are non-dimensionalized, the resulting system is analyzed using analytic and numeric techniques. Six different parameters are considered and their effects on the velocity of propagation of the traveling fronts are investigated. Based on the numerical solutions obtained, the most important parameter that allows the immune cells to overtake the spreading bacteria is the activation rate of the immune cells. However, there seemed to be no regiment of parameters under which the bacteria were totally exterminated.

Introduction

Lyme disease in humans

Lyme disease is a rapidly emerging infectious disorder caused by the tick-borne spirochaetal bacterium *Borrelia burgdorferi*. Since it was first identified in the 1970s, the incidence of Lyme disease has increased more than thirty-fold and is now considered the most prevalent arthropod- transmitted infection in both the USA and Europe (Radolf, Salazar and Dattwyler 487), allowing it to be considered as the prototype of an emerging infectious disease. The genome of *B. burgdorferi* bears resemblance to that of syphilis and the agents of the relapsing fever, but it is sufficiently distinct to merit designation as a separate species (Hyde and Johnson). If untreated, Lyme disease can lead to a wide array of complications typically involving the heart, joints, or nervous system. Arguably the most dangerous consequence of Lyme disease is the possibility of cardiac blocks, which can cause people with cardiomyopathy to experience the storms of ventricular tachycardia, which, if not averted, in the course of several minutes will result in cardiac arrest and subsequent death.

During the first several days after the inoculation, spirochaetes establish a foothold and begin to replicate, with the population eventually growing large enough that they are relatively easy to detect by either culture or polymerase chain reaction (Radolf, Salazar and Dattwyler 498). Laboratory tests are not the only way to detect the presence of Lyme disease. In fact, in humans, for every third person, one of the first manifestations of Lyme disease is a roughly circular-shaped rash known as Erythema Migrants (EM) that appears within 7-14 days after the tick detaches from the skin and then spreads at a rate of approximately 20 cm^2 per day (Radolf, Salazar and Dattwyler 508). In some cases, there is central clearing in the EM rash, resembling a bull's-eye pattern, which is considered the hallmark of Lyme disease in North America. At the

time of writing this thesis, the exact cause of such an inflammatory rash remains uncertain, but it is likely caused by the host immune response to the bacterial infection. Once diagnosed, antibiotics are the most common way of battling the infection. The medical community also reminds people that the presence of Lyme anti-bodies does not rule out the possibility of reinfection, which could happen due to either relapse or a new instance of being bitten by an infected tick. Moreover, for an EM to be recurrent, it has to occur at the same site as the original infection within a relatively short time interval (Radolf, Salazar and Dattwyler 514).

The costs associated with the diagnosing and subsequent managing of Lyme disease are high. In fact, when direct medical expenses are combined with indirect costs (non-medical cost and productivity loss), the economic Lyme-evoked damages approach $230 million in the USA alone (Marconi and Earnhart 468). With such a large impact on human welfare, the advancement of Lyme disease research holds the promise of improving the wellbeing of many people throughout the world.

One dimensional diffusion

When modeling the motion of a bacterial organism in some medium, be it a liquid or a gas, it is natural to think of the trajectory of its motion as a random walk. These "drunkard's" walks are diffusive in nature, and therefore they can be adequately modeled using a diffusion equation.

Diffusion describes the random process of particles spreading down the concentration gradient. The simplest case of diffusion is a one dimensional dispersion of particles which demonstrates that the time rate of change of a certain quantity b is proportional to its second spatial derivative as expressed below:

$$\frac{\partial b}{\partial t} = D \frac{\partial^2 b}{\partial x^2}. \tag{1}$$

The equation above is a one dimensional, parabolic, partial differential equation and D is a constant. In physics, this equation is widely used when modeling phenomena such as heat transfer through an object or diffusion of particles in a medium (hence D is called a diffusion coefficient or the diffusivity). This equation is usually considered for x in some fixed interval $0 \leq x \leq L$, with a boundary condition of $b(x,0) = f(x)$ along with respective boundary conditions at the endpoints for all $t \geq 0$.

If we consider an equally spaced grid we can easily arrive at the following approximation of (1):

$$\frac{b(x, t + \Delta t) - b(x, t)}{\Delta t} = D \frac{b(x + \Delta x, t) - 2b(x, t) - b(x - \Delta x, t)}{\Delta x^2}. \tag{2}$$

Employing index notation allows us to express (2) in a much simpler form:

$$\frac{b_{i,j+1} - b_{i,j}}{\Delta t} = D \frac{b_{i+1,j} - 2b_{i,j} - b_{i-1,j}}{\Delta x^2}. \tag{3}$$

Multiplying both sides of (3) by Δt and combining like terms results in:

$$b_{i,j+1} = (1 - 2\lambda)b_{i,j} + \lambda(b_{i+1,j} - b_{i-1,j}) \tag{4}$$

where $\lambda = D\Delta t/\Delta x^2$.

Having such an expression for λ is quite restrictive, for in order to achieve sufficient accuracy, Δx has to be small, which forces Δt to be very small. Indeed, decreasing the value of the spatial resolution (Δx) by a factor of $1/n$ will also increase by a factor of n the number of time steps needed to reach a certain t-value. Furthermore, the expression for λ reveals that we should not make the system move too fast along the t-axis and thus we should consider choosing small Δt. It can also be shown that choosing $\lambda \leq 1/2$ is crucial to the convergence of the method for when $\lambda = 1/2$, the $b_{i,j}$ terms vanish from (4) and for $\lambda < 1/2$, the $b_{i,j}$ terms have positive coefficients in (4). Adherence to the condition imposed on the value of λ makes this approach conditionally stable. The following method is based on a more satisfactory discretization of the diffusion equation.

Crank-Nicolson method

In the mid 20th century John Crank and Phyllis Nicolson devised a method that imposes no restrictions on λ, making this method unconditionally stable. It uses values of b at six different points and can be visualized by Figure1.
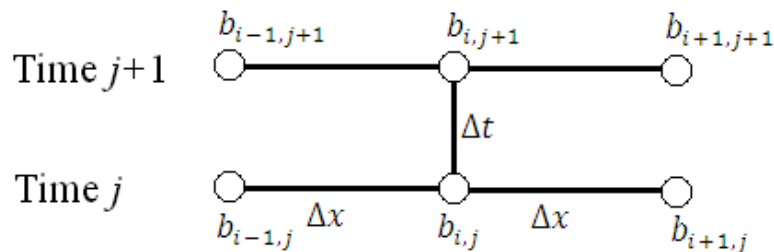

Figure 1. The six points in the Crank-Nicolson method.

The mathematical idea behind this method entails averaging the approximations for the time derivative found by the forward Euler method and backward Euler method as shown in the following three equations.

$$\frac{b_{i,j+1} - b_{i,j}}{\Delta t} = D \left(\frac{b_{i+1,j} - 2b_{i,j} + b_{i-1,j}}{\Delta x^2} \right) \qquad \text{Forward Euler method.}$$

$$\frac{b_{i,j+1} - b_{i,j}}{\Delta t} = D \left(\frac{b_{i+1,j+1} - 2b_{i,j+1} + b_{i-1,j+1}}{\Delta x^2} \right) \qquad \text{Backward Euler method.}$$

$$\frac{b_{i,j+1} - b_{i,j}}{\Delta t} = \frac{D}{2} \left[\frac{b_{i+1,j} - 2b_{i,j} + b_{i-1,j}}{\Delta x^2} + \frac{b_{i+1,j+1} - 2b_{i,j+1} + b_{i-1,j+1}}{\Delta x^2} \right] \qquad (5)$$

Multiplying both sides of (5) by $2\Delta t$, writing $\lambda = D\Delta t/\Delta x^2$ as before, and collecting the three

terms corresponding to time row $j+1$ on the left yields:

$$(2 + 2\lambda)b_{i,j+1} - \lambda\left(b_{i+1,j+1} + b_{i-1,j+1}\right) = (2 - 2\lambda)b_{i,j} + \left(b_{i+1,j} + b_{i-1,j}\right). \quad (6)$$

In general, the three values on the left are unknown, and the three values on the right are known

(Kreyszig 1099).

If we divide the x interval $0 \leq x \leq L$ into n equal intervals, we will then have $n - 1$

internal mesh points per time row. Next, using (6) for $j = 0$ and $i = 1, \ldots, n - 1$, we will obtain a

system of $n - 1$ linear equations for the $n - 1$ unknown values $u_{1,1}, u_{2,1}, \ldots, u_{n-1,1}$ in the first time

row which will be expressed in terms of the initial values $u_{0,0}, u_{1,0}, \ldots, u_{n,0}$ and the boundary

values $u_{0,1}, \ldots, u_{n,1}$. The algorithm is then repeated for each time row, that is, for $j = 1$ to

$j = n - 1$, and we must solve such a system of $n - 1$ linear equations resulting from (6).

Although the numerical value of λ is no longer restricted, choosing smaller values of Δt

will still result in better accuracy of the results.

Model

The seminal event in the natural progression of Lyme disease is the deposition of spirochaetes into the skin. The actual inoculation delivered by ticks has not been precisely measured but available evidence suggests that it is small (Radolf, Salazar and Dattwyler 497). Hence, when constructing the model, we assumed that the initial deposition of the bacteria is not exceeding several hundred spirochaetes.

When creating the model, the main principles were borrowed from the Keller-Segel system for chemotaxis that describes the collective motion of cells. It was assumed that the bacteria can spread (diffuse) from the regions with higher concentration to regions with lower concentration. It was also asserted that the *B. burgdorferi* bacteria grow proportionally to their population and that they become deactivated proportionally to the number of macrophages present. When it comes to diffusion, macrophages act in an opposite fashion to that of the bacteria, that is, the macrophages move from the segment with the lower concentration of bacteria to where the bacteria are more concentrated. In other words, the bacteria wants to diffuse away from the inoculation site while the macrophages exhibit the affinity to converge to the place where bacteria is most concentrated. This fact is accounted for by having a minus sign in front of the diffusion term of the macrophages. Unlike the bacteria, the macrophages do not grow and multiply but rather are assumed to be dormant and become activated in response to the presence of the bacteria. The number of activated macrophages is assumed to be proportional to the concentration of the bacteria. Similarly, macrophages are assumed to engage in phagocytosis, which leads to their deactivation. The likelihood of a macrophage becoming inactive is assumed to be proportional to the overall concentration of macrophages. By considering the aforementioned assumptions, a mathematical model was postulated and is presented below:

$$\frac{\partial b}{\partial t} = D\frac{\partial^2 b}{\partial x^2} + \sigma_b b - \gamma_b mb$$

$$\frac{\partial m}{\partial t} = -\frac{\partial}{\partial x}\left(\chi m\frac{\partial b}{\partial x}\right) + \sigma_m b - \gamma_m m \,. \tag{7}$$

In system (7) the bacteria (with density b) diffuse, replicate at rate σ_b, and are destroyed by the immune cells with rate $\gamma_b m$. The immune cells chemotax toward the bacteria with velocity $\chi\,\partial b/\partial x$, are activated at rate $\sigma_m b$, and are deactivated with rate γ_m. As the EM rash spreads at a roughly constant rate (Radolf, Salazar and Dattwyler 508), it was suspected that the system might have a traveling front solution -- a hypothesis which found support in the accompanying computer simulations. However, in order for the equations to be solved numerically, we discretized the system of equations in space and time such that $b_{i,j}$ is the bacterial density at node $i\Delta x$ at time $j\Delta t$. The time derivatives are then discretized as:

$$\frac{\partial b_{i,j}}{\partial t} \approx \frac{b_{i,j+1} - b_{i,j}}{\Delta t} \tag{8}$$

with an analogous expression for m. A pseudo-implicit scheme based off of the Crank-Nicolson method was constructed. The first equation in (7) becomes:

$$\left(1+\tilde{D}-\frac{\tilde{\sigma}_b}{2}\right)b_{i,j+1} - \frac{\tilde{D}}{2}b_{i+1,j+1} + b_{i-1,j+1} = \left(1-\tilde{D}+\frac{\tilde{\sigma}_b}{2}\right)b_{i,j} + \frac{\tilde{D}}{2}b_{i+1,j} + b_{i-1,j} - \tilde{\gamma}_b m_{i,j} b_{i,j} \tag{9}$$

where $\tilde{D} = D\Delta t/\Delta x^2$, $\tilde{\sigma}_b = \sigma_b \Delta t$, and $\tilde{\gamma}_b = \gamma_b \Delta t$.

A stable way to develop the dynamic algorithm for the immune cells was to write a discretization of the second equation in (7) as:

$$1+\tilde{\chi}B_1+\tilde{\gamma}_m\ m_{i,j+1}+\tilde{\chi}B_2 m_{i+1,j+1}-\tilde{\chi}B_3 m_{i-1,j+1} = 1-\tilde{\chi}B_1-\tilde{\gamma}_m\ m_{i,j}-\tilde{\chi}B_2 m_{i+1,j}+\tilde{\chi}B_3 m_{i-1,j}+\tilde{\sigma}_m b_{i,j} \tag{10}$$

where

$$B_1 = b_{i+1,j} - 2b_{i,j} + b_{i-1,j}$$
$$B_2 = b_{i+1,j} - b_{i,j}$$
$$B_3 = b_{i,j} - b_{i-1,j}$$
$$\tilde{\chi} = \frac{\chi \Delta t}{4 \Delta x} \tag{11}$$
$$\tilde{\sigma}_m = \sigma_m \Delta t$$
$$\tilde{\gamma}_m = \frac{\gamma_m \Delta t}{2}$$

This discretization comes from a finite volume approach to the second equation of (7) and uses a Crank-Nicolson scheme.

Also, to ensure the stability of our computer code we introduced a small amount of regular diffusion for macrophages in the second equation of (7). After accounting for the introduction of the diffusion term into the second equation of (7), (10) becomes:

$$-\left(XB_3 + \frac{L}{2}\right)m_{i-1,j+1} + (1 + L + XB_1 + \gamma_m)m_{i,j+1} + \left(XB_2 + \frac{L}{2}\right)m_{i+1,j+1} =$$
$$\left(XB_3 + \frac{L}{2}\right)m_{i-1,j} + (1 - L - XB_1 - \gamma_m)m_{i,j} - \left(XB_2 - \frac{L}{2}\right)m_{i+1,j} + \sigma_m b_{i,j} \tag{12}$$

where $L = k\Delta t/\Delta x^2$ and $k = 0.01$.

Computational software MATLAB by MathWorks was used to implement (9) and (12) (see the Appendix for the actual code). Once implemented, the algorithm was used to investigate the effects of the six parameters (γ_m, γ_b, χ, σ_m, σ_b, D) on the time evolution of the position of peak concentrations for both species.

The results of the computer simulations were tabulated, graphed and are presented and discussed in the following section.

Results and discussion

One unit of time in our simulation is approximately equivalent to 1 day, while one unit of length signifies a millimeter. To measure the effect of the aforementioned parameters on the velocity of the traveling peaks, both r and t were chosen large enough to prevent the traveling fronts from "wrapping around" (reaching the boundary of the simulation and appearing on the opposite side of the x-axis). For this purpose, all of the simulations were conducted on the domain with $r = 100$ (radius of 10 cm) for durations of either $t = 10$ or $t = 20$.

For each set of simulations, MATLAB was used to generate the numerical solutions, which were then graphed and interpolated (linearly) in Microsoft Excel. The results of interpolation were used to determine the speeds of the traveling fronts. All of the numerical values for the speeds were systematically tabulated and graphed using either regular or logarithmic scales.

In the course of the simulation, we were mindful that every time peaks drifted away from the center, we were in effect looking at the spreading of the fringes of the "bull's-eye" rush. However, our model has always resulted in some sort of EM, be it a stationary peak at the origin or a multiple train of peaks with dampened amplitudes.
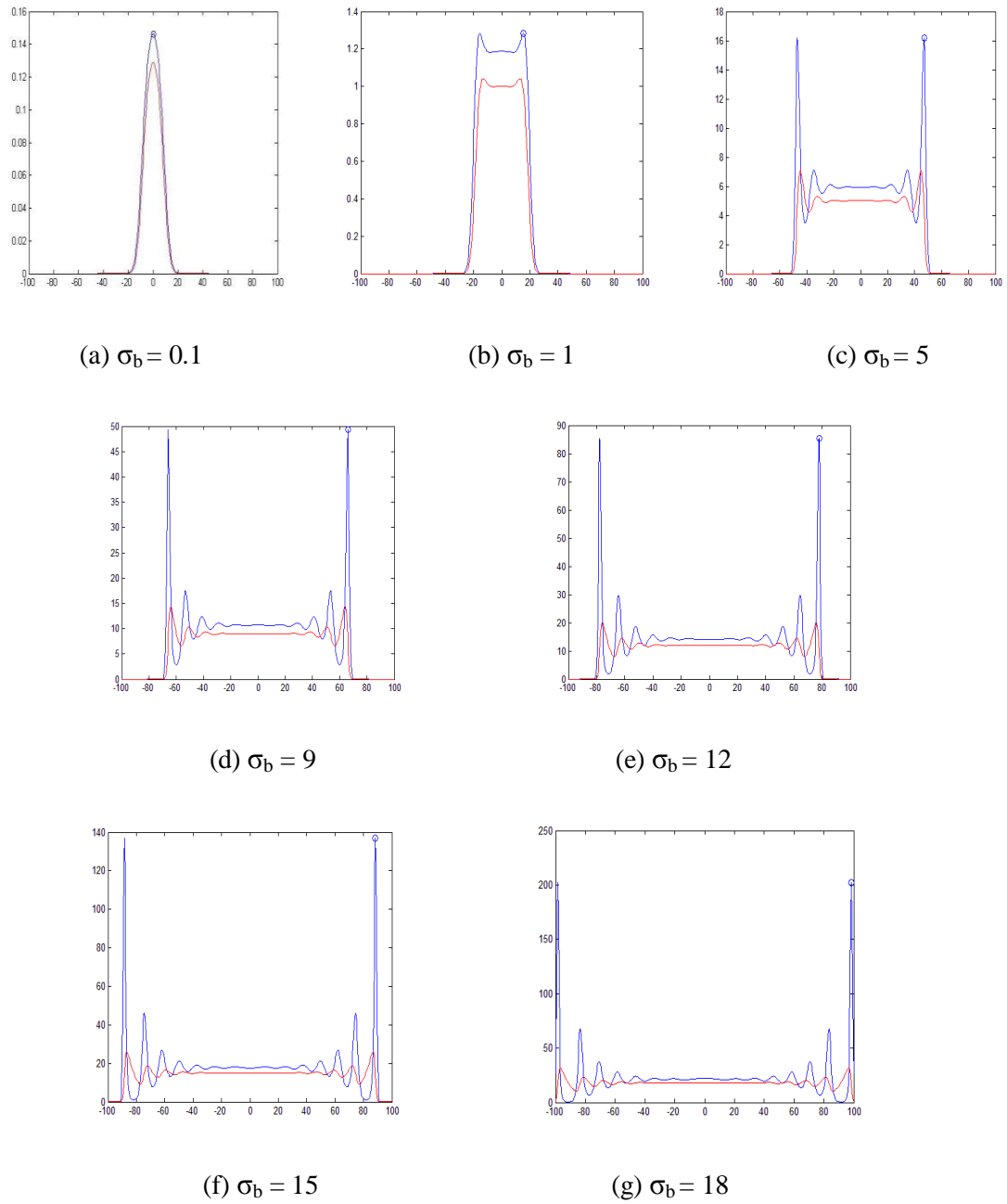
Effect of the bacterial growth rate on dx/dt

For the six parameters considered, our system was the most sensitive to changes in the growth rate (σ_b) of the bacteria. As seen from Graph 1 and Figure 2, varying σ_b affects the values of stable states, frequency and velocities of the peaks. When analyzing the plot of σ_b versus the velocity, we found that, for the most part, before the peaks reach the end points of the domain, we can reasonably approximate their velocity with a polynomial of 6th degree. However, it appears that there are no values of σ_b that would allow the macrophages to overtake the spreading bacteria.
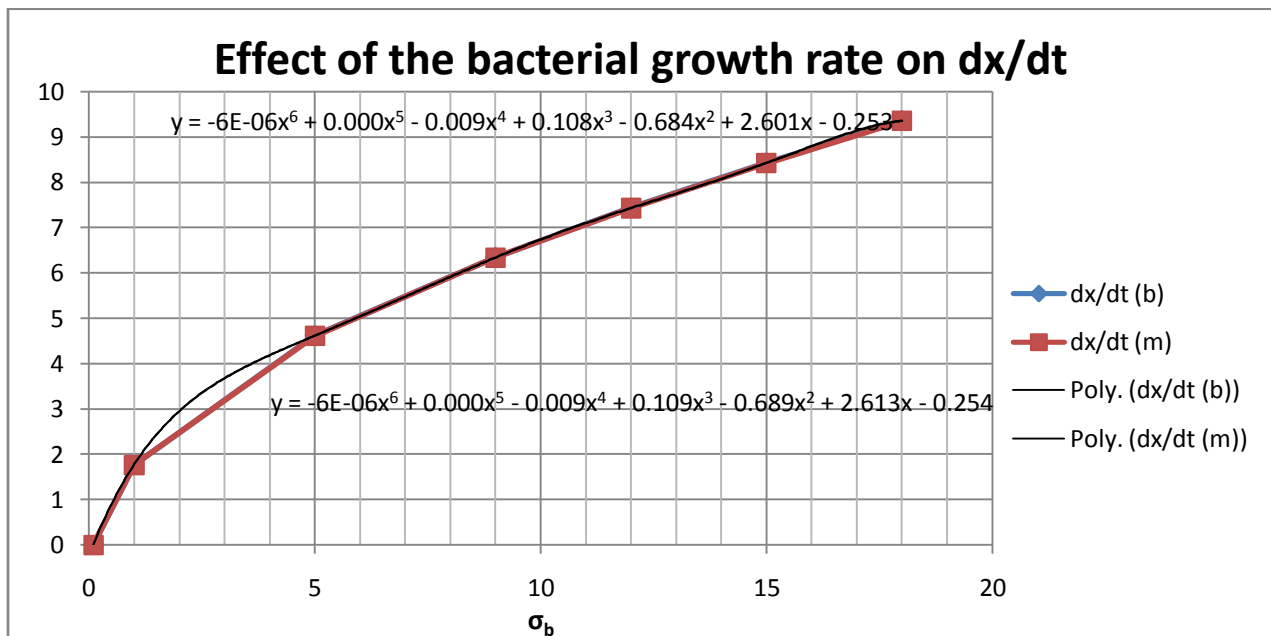
Graph 1. Effect of the bacterial growth rate (σ_b) on dx/dt.

σ_b	dx/dt (b)	dx/dt(m)
0.1	0	0
1	1.77	1.763
5	4.62	4.612
9	6.347	6.336
12	7.439	7.427
15	8.434	8.423
18	9.365	9.352

Table 1. Numerical data used for generating Graph 1.

(a) $\sigma_b = 0.1$ (b) $\sigma_b = 1$ (c) $\sigma_b = 5$

(d) $\sigma_b = 9$ (e) $\sigma_b = 12$

(f) $\sigma_b = 15$ (g) $\sigma_b = 18$

Figure 2. Concentrations of macrophages (red) and bacteria (blue) at $t = 10$.

Effect of the deactivation rate of macrophages on dx/dt

When γ_m was set to 1, the macrophages come close to catching up with the bacteria. At the same time, there was a modest secondary peak that caused another wave of the macrophages to spread, thus closely resembling the spread of the EM. With $\gamma_m = 0.01$, the macrophages grow steadily and rapidly reach three-fold the concentration of the bacteria. Also, there is a secondary peak that tends to linger and not spread out.

With $\gamma_m = 5$, the bacteria feels quite at home and the peaks of both concentrations do not move away from the origin (Figure 3 d, e). For any $\gamma_m > 2.5$, the resulting velocity of the peaks are zero.
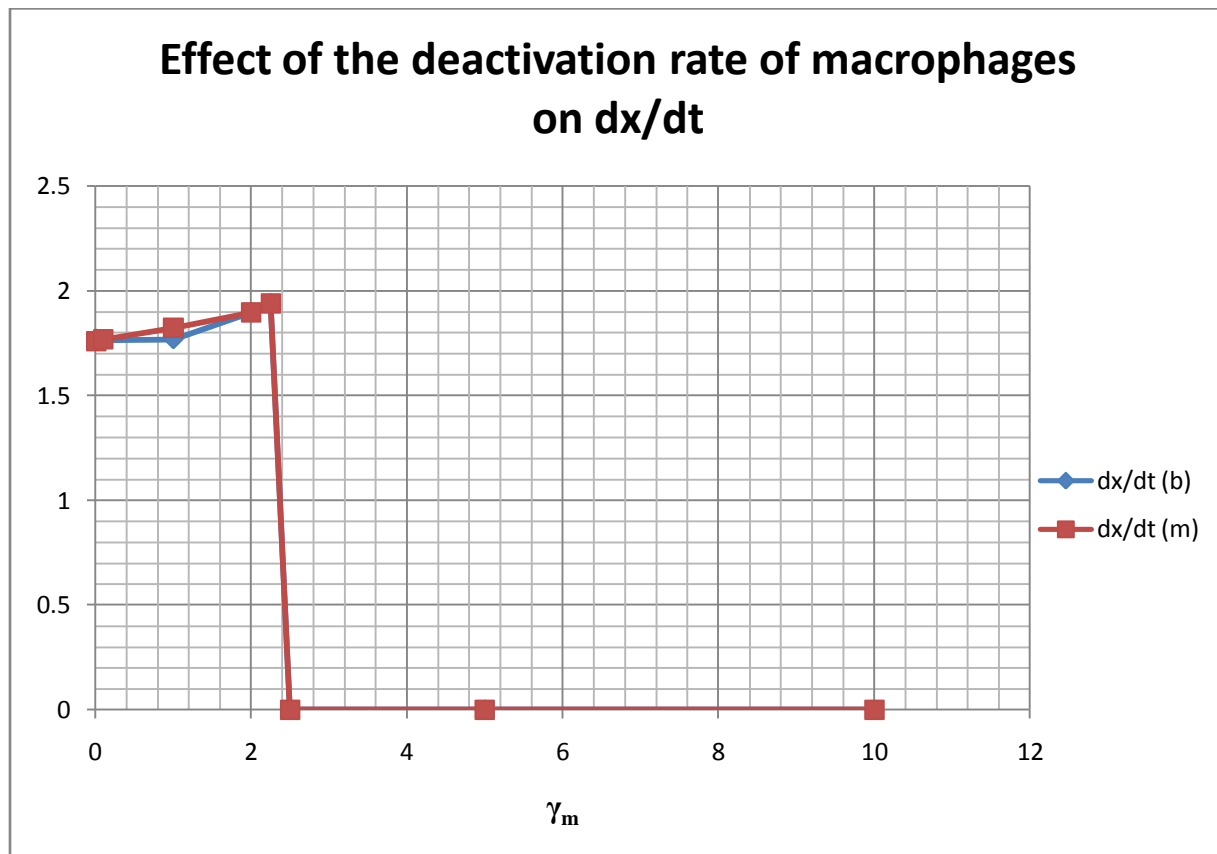
Graph 2. Effect of the deactivation rate of macrophages (γ_m) on dx/dt.

γm	dx/dt (b)	dx/dt (m)
0.01	1.77	1.76
0.1	1.766	1.767
1	1.769	1.823
2	1.897	1.897
2.25	1.939	1.939
2.5	0	0
5	0	0
10	0	0
40	0	0

Table 2. Numerical data used for generating Graph 2.

(a) $\gamma_m = 0.1$ (b) $\gamma_m = 1$ (c) $\gamma_m = 3$

(d) $\gamma_m = 5$ (e) $\gamma_m = 40$
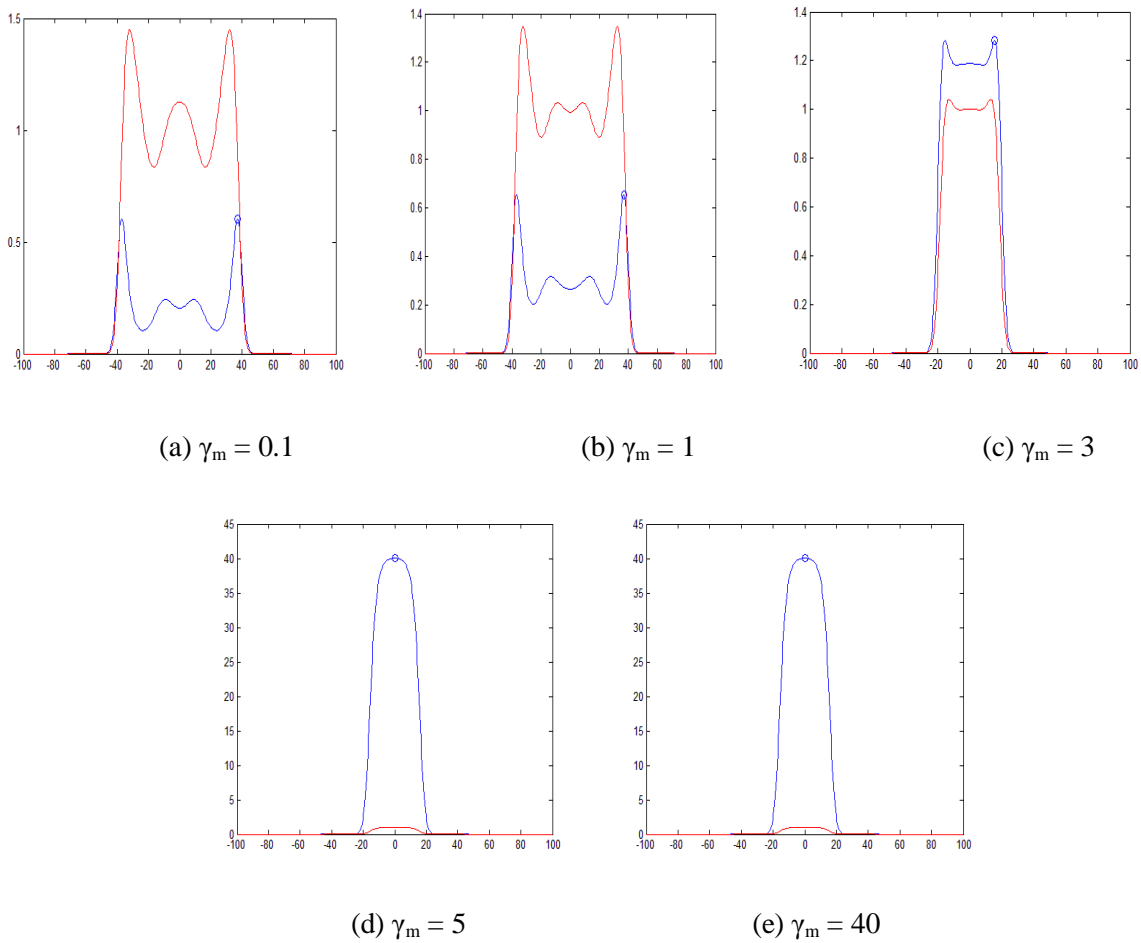
Figure 3. Concentrations of macrophages (red) and bacteria (blue) at $t = 10$.

Effect of macrophage chemotaxis on dx/dt

Nine different values were considered for the chemotaxis (χ) of macrophages and it was found that in each case the peaks of both the bacteria and the macrophages were moving away from the origin of the inoculation at a persistently constant speed.
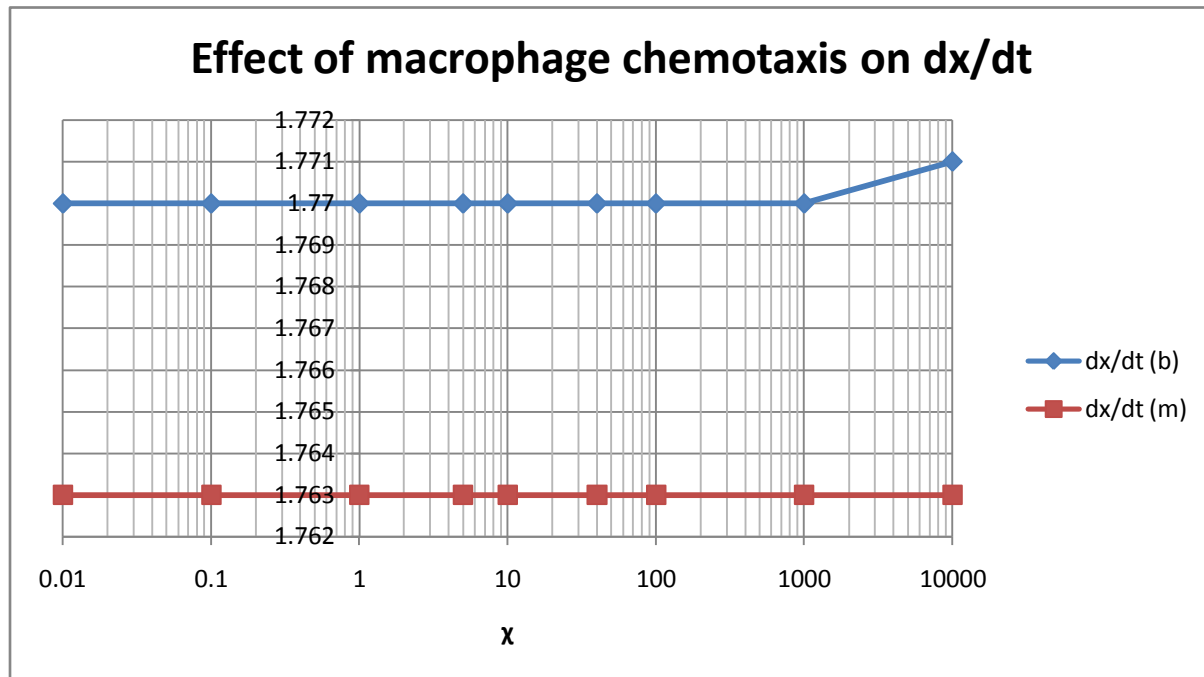
Graph 3. Effect of macrophage chemotaxis (χ) on dx/dt.

χ	dx/dt (b)	dx/dt (m)
0.01	1.77	1.763
0.1	1.77	1.763
1	1.77	1.763
5	1.77	1.763
10	1.77	1.763
40	1.77	1.763
100	1.77	1.763
1000	1.77	1.763
10000	1.771	1.763

Table 3. Numerical data used for generating Graph 3.

(a) χ = 0.1 (b) χ = 1 (c) χ = 5

(d) χ = 5 (e) χ = 10 (f) χ = 40

(g) χ = 100 (h) χ = 1000 (i) χ = 10000
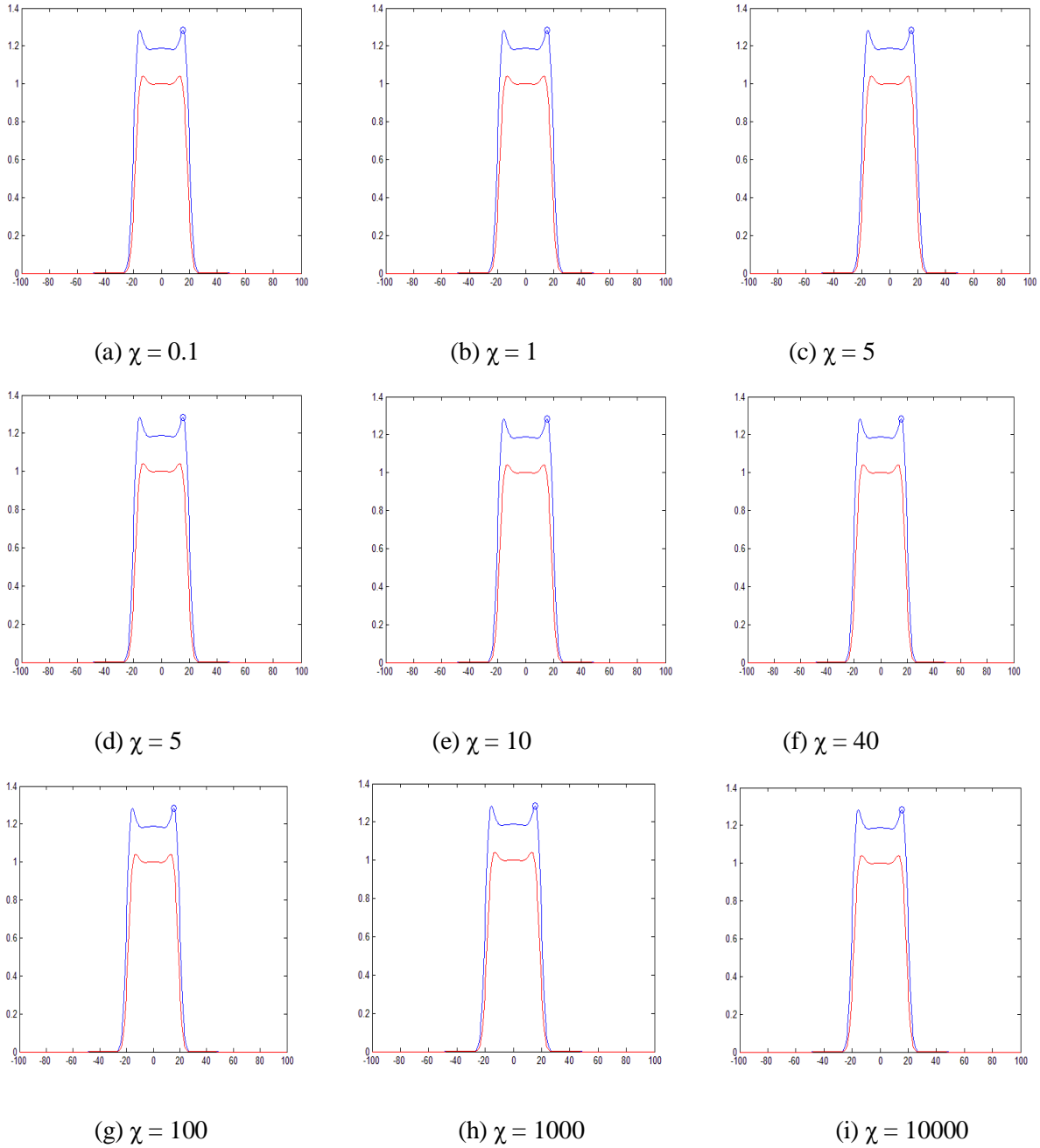
Figure 4. Concentrations of macrophages (red) and bacteria (blue) at $t = 10$.

As evident from both Graph 3 and Figure 4, qualitative behavior of both populations remained virtually the same for χ ranging from 10^{-2} to 10^{4}.

Effect of the killing rate on dx/dt

Nine different values were tried and in each case the qualitative behavior of the solutions was virtually the same. In each case the concentration of the macrophages was inferior to that of the bacteria. The bacteria showed only one initial peak (at the inoculation site), which swiftly split into two peaks moving in the opposite direction. The macrophages followed suit with both concentrations reaching the steady state as shown in the figures below.

	b	m
γ_b	dx/dt	dx/dt
0.1	1.951	1.951
1	1.919	1.918
5	1.908	1.905
10	1.905	1.903
20	1.903	1.901
30	1.901	1.899
40	1.901	1.898
100	1.899	1.896
1000	1.895	1.892
10000	1.894	1.892

Table 4. Numerical data used for generating Graph 4.
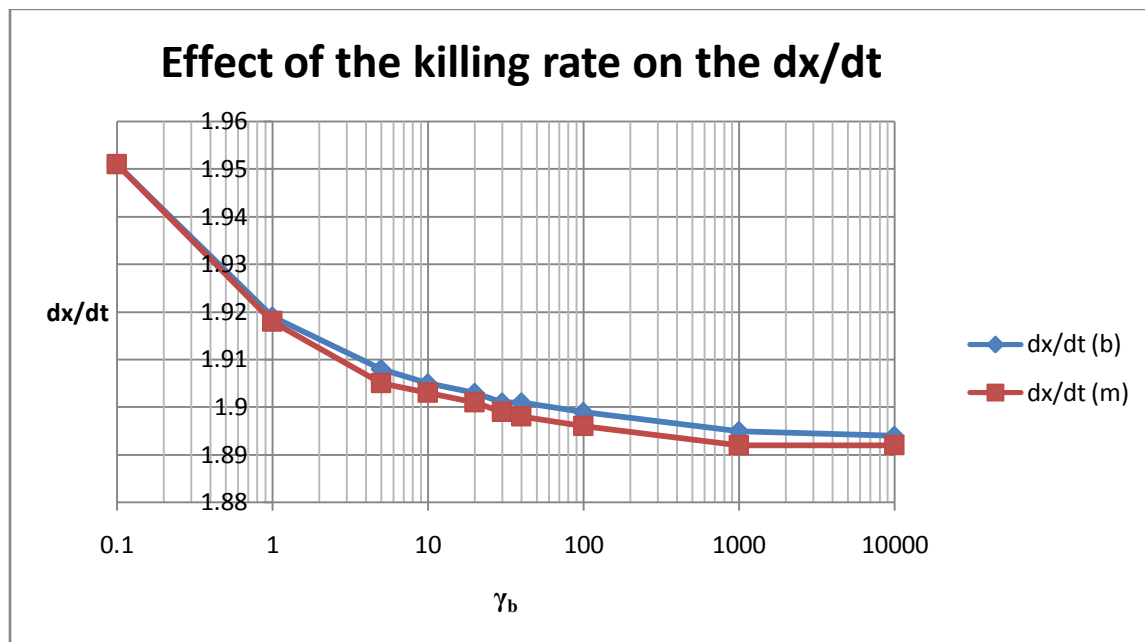
Graph 4. Effect of activation rate for the macrophages (γ_b) on dx/dt.

With $\gamma_b = 0.1$, the bacteria grows relatively slowly and the macrophages respond at an even slower rate. Every time the value of γ_b was increased ten-fold, the picture was a duplicate of that with $\gamma_b = 0.1$. All this time the bacteria has been spreading faster and further than the macrophages, which have to play catch-up. With $\gamma_b = 10$ there was still no secondary peak but with $\gamma_b = 20$ the macrophages were able to briefly overtake the vertical peak of the bacteria at the

center. However, such dominance is short lived and the concentration of the macrophages decreases rapidly which leads to the backlash of the bacteria at the area of inoculation, thus leading to the secondary peak in the concentration of the pathogen.

With $\gamma_b = 1000$, the bacteria at the center gets severely suppressed which causes the initial hump to split into two almost immediately after the inoculation. When $\gamma_b = 10000$, the bacteria gets dramatically suppressed by the relatively large and extremely aggressive population of macrophages. However, the balance of power shifts very quickly and at $t = 10$ the macrophages are not only outnumbered but they also trail significantly behind the spreading front of bacteria.
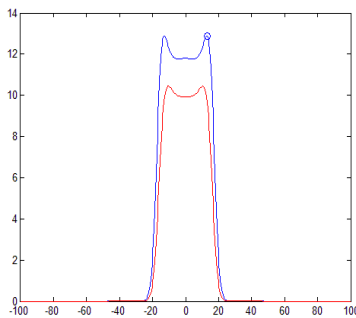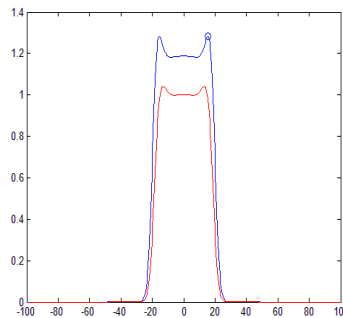
(a) $\gamma_b = 0.1$ (b) $\gamma_b = 1$ (c) $\gamma_b = 5$
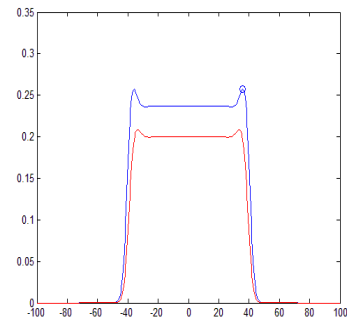
(d) $\gamma_b = 10$ (e) $\gamma_b = 20$ (f) $\gamma_b = 40$
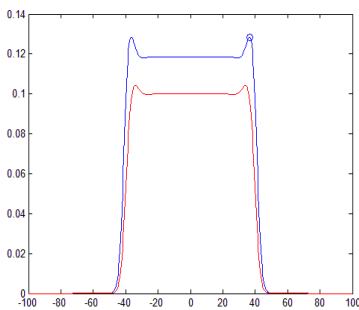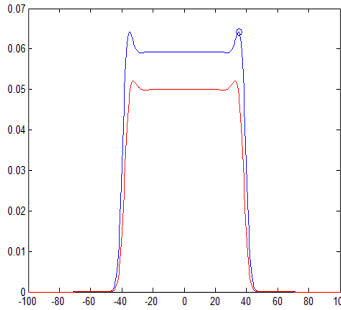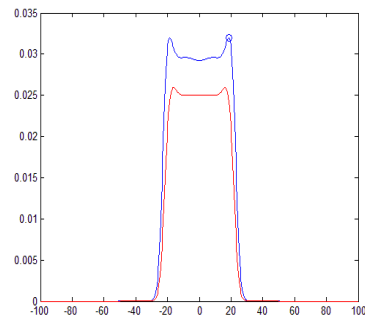
(g) $\gamma_b = 100$ (h) $\gamma_b = 1000$ (i) $\gamma_b = 10000$
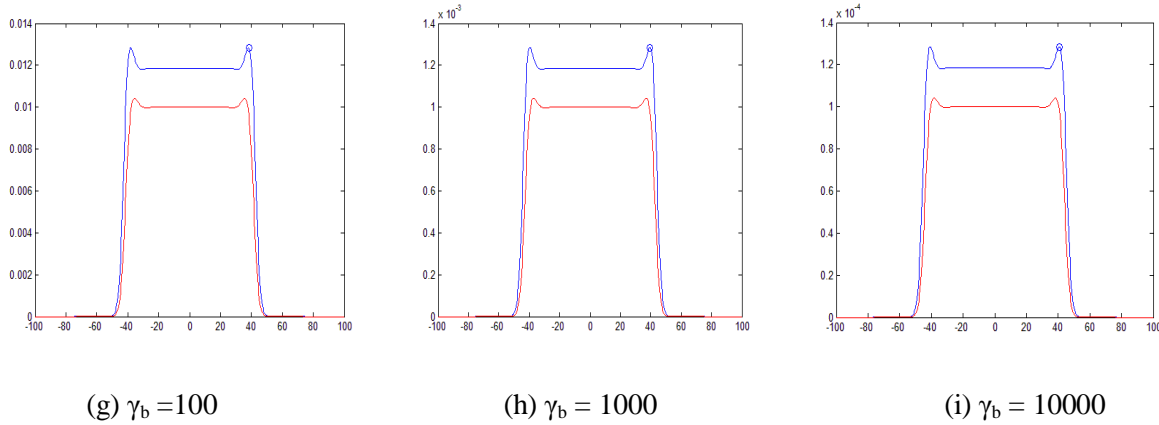
Figure 5. Concentrations of macrophages (red) and bacteria (blue) at $t = 10$.

The levels of the steady state (time derivatives are zero) could also be predicted by discarding the

nonlinearities from system (7):

$$0 = \sigma_b b - \gamma_b mb$$

$$0 = \sigma_m b - \gamma_m m$$

which means that $m = \sigma_b / \gamma_b$ and $b = \sigma_b \gamma_m / \sigma_m \gamma_b$. Indeed, with all of the parameters being set to

1, the macrophages' analytical and graphical settling levels match exactly. If the simulation were

to be conducted for a considerably longer time period ($t \gg 10$) then the level of bacteria would

be expected to decrease to the theoretically predicted levels. However, based on the data

presented in both Graph 4 and Figure 5, it was concluded that enhancing the rate of the

macrophages' phagocytizing does not enable the concentration peak of the macrophages to

overtake that of the bacteria.

Effect of diffusion of bacteria on dx/dt

Next we considered the effect of changes in the diffusivity of the bacteria. It was found that varying D_b had no effect on the steady state levels of concentrations, which seems to suggest that even when the bacteria is highly hyper and diffusive, this does not pose an impediment for macrophages to regulate the concentration of the infection. On the other hand, even "sleepy" bacteria with very low ability to diffuse will still be able to evade complete extermination by the immune system.

	b	m
D_b	dx/dt	dx/dt
0.1	0.875	0.887
1	1.81	1.789
5	3.88	3.859
10	5.54	5.572
20	8.001	8.211
30	10	10.48
40	11.88	12.74

Table 5. Numerical data used for generating Graph 5.

As can be seen from Graph 5, increasing D_b resulted in an increase in the speed of propagation of the bacteria, and, as a reaction, the macrophages' velocity increased. Also, out of all variables analyzed, we were able to obtain an extremely precise approximation polynomial to express the velocity of the traveling front as a function of D_b.
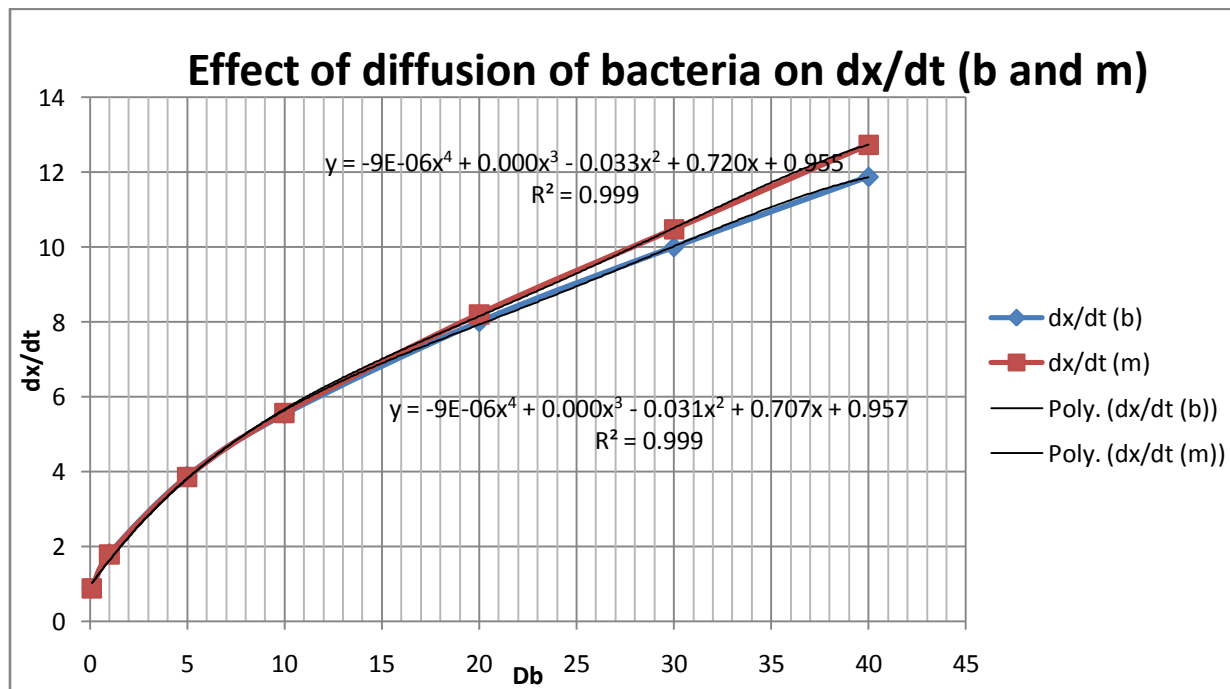

Graph 5. Effect of diffusion of bacteria on dx/dt.
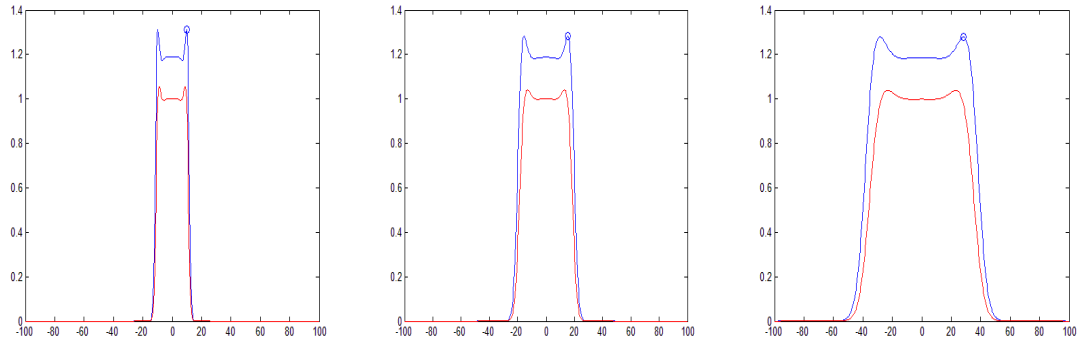
(a) $D_b = 0.1$ (b) $D_b = 1$ (c) $D_b = 5$
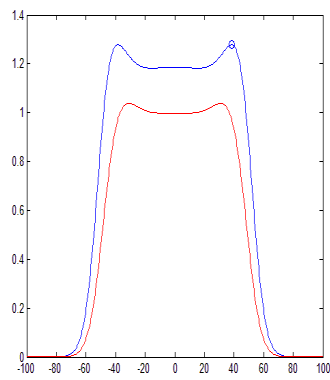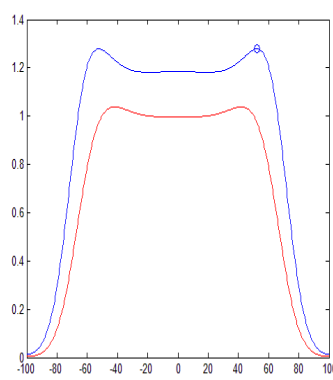
(d) $D_b = 10$ (e) $D_b = 20$
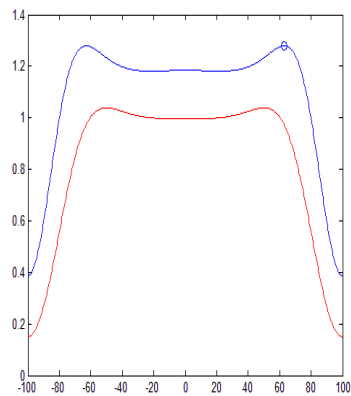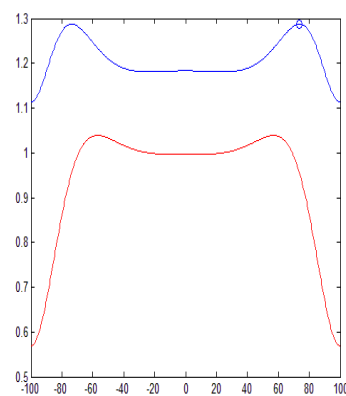
(f) $D_b = 30$ (g) $D_b = 40$

Figure 6. Concentrations of macrophages (red) and bacteria (blue) at $t = 10$.

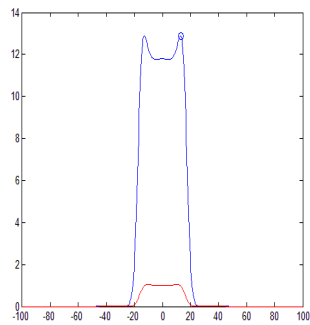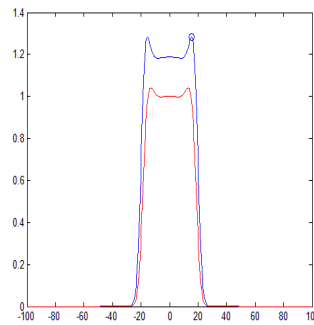## Effect of activation rate for macrophages on dx/dt

In the course of experimentation with the various parameters of our model, we found that the "Holy Grail" of enabling the immune cells to both overtake the peak and significantly reduce the concentration of the bacteria is the value of the activation rate of the macrophages (σ_m). Our numerical results suggested that the peaks of macrophages are far from consistent in moving faster than that of the bacteria. This occurrence can be explained by the fact that during simulations, the MATLAB code was fine-tuned to track the movement of the peak of the bacteria concentration; hence Graph 6 shows accurately the velocities of the peaks, however small their amplitude may be. However, as shown in parts a-i of Figure 7, it is clear that the increase in σ_m yields consistent qualitative behavior which might be the most desirable qualitative behavior when trying to design a means to treat the spread of the infection.
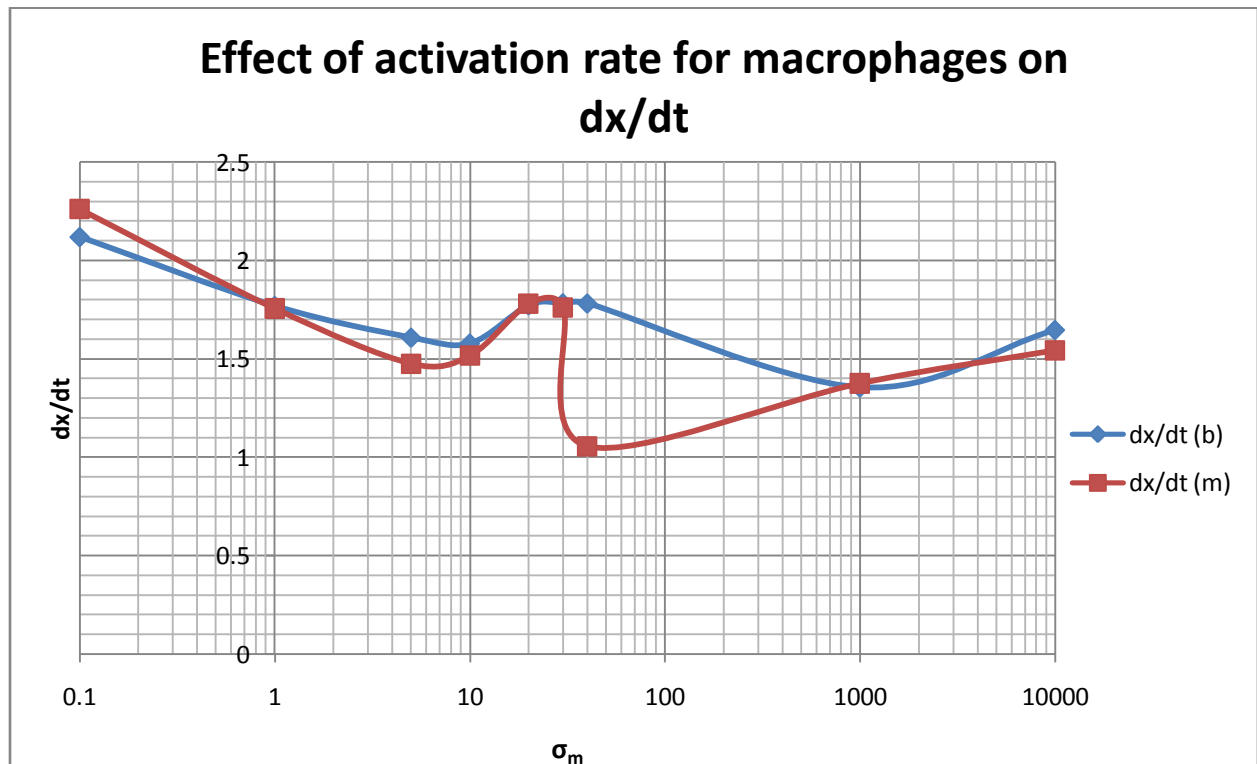
Graph 6. Effect of activation rate for the macrophages (σ_m) on dx/dt.

	b	m
σ_m	dx/dt	dx/dt
0.1	2.12	2.261
1	1.769	1.756
5	1.608	1.476
10	1.578	1.517
20	1.773	1.781
30	1.783	1.761
40	1.782	1.056
1000	1.355	1.376
10000	1.647	1.544

Table 6. Numerical data used for generating Graph 6.

(a) $\sigma_m = 0.1$ (b) $\sigma_m = 1$ (c) $\sigma_m = 5$
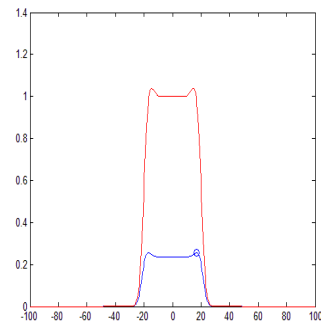
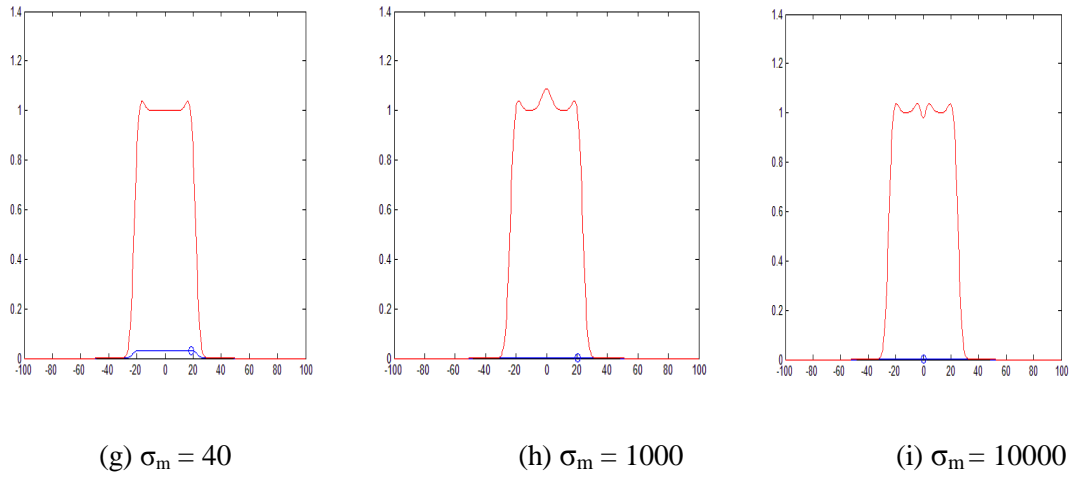(d) $\sigma_m = 10$ (e) $\sigma_m = 20$ (f) $\sigma_m = 30$
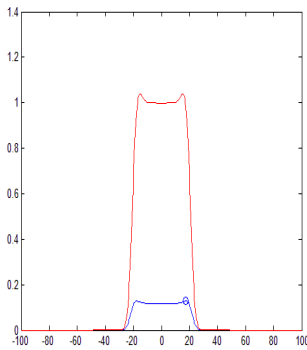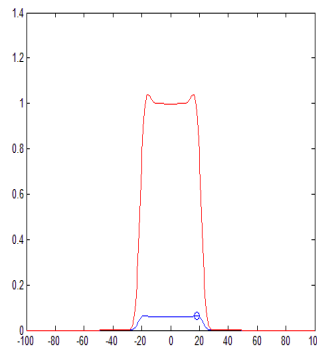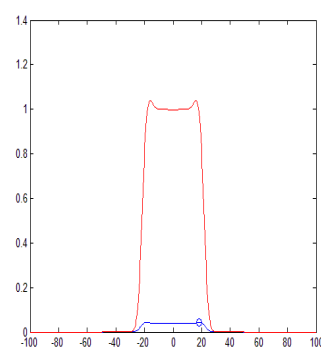
(g) $\sigma_m = 40$ (h) $\sigma_m = 1000$ (i) $\sigma_m = 10000$

Figure 7. Concentrations of macrophages (red) and bacteria (blue) at $t = 10$.

Conclusion and Future Work

Lyme disease, which is caused by the spirochete *Borrelia burgdorferi*, is the most common tick-transmitted illness in the United States. This project has shown that the immune cells' response to the *B. burgdorferi* can be described mathematically when using the Keller-Segel model for chemotaxis. Based on our findings, in order to ensure that the velocity of the spreading concentration of macrophages is greater than that of the bacteria, we must develop a mechanism for enhancing the activation rate of macrophages.

Based on our numerical results, it is reasonable to suppose the existence of a traveling front solution, and hence, a part of the future work would be to try and solve the system analytically. Once finished analyzing the 1D problem, the next step is to consider a 1D cylindrically-symmetric model, as well as a transition to a 2D model and eventually to a 3D model.

Works cited

Hyde, F.W., and Johnson, R.C. (1984). Genetic relationship of Lyme disease spirochetes to

    Borrelia, Treponema, and *Leptospira* ssp. J. Clin. Microbiol. 20, 151-154.

Kreyszig, Erwin, <u>Advanced Engineering Mathematics 6th Edition</u>, New York, John Wiley &

    Sons, Inc. 1988.

Radolf, Justin D., Salazar, Juan C., and Dattwyler, Raymond J. Lyme Disease in Humans,

    <u>Borrelia: Molecular Biology, Host Interaction and Pathogenesis</u>. Ed. Samuels, D.S. and

    Radolf, J.D., Norfolk, UK, Caister Academic Press, 2010.

Marconi, Richard T., and Earnhart, Christopher G. Lyme Disease Vaccines, <u>Borrelia: Molecular</u>

    <u>Biology, Host Interaction and Pathogenesis</u>. Ed. Samuels, D.S. and Radolf, J.D., Norfolk,

    UK, Caister Academic Press, 2010.

Appendix

MATLAB code

```matlab
function [xpeak] = BorreliaInfect1D(chi)

%% define biological parameters

Db = 1;      %% diffusion coefficient for bacteria*;
sigb = 1;   %% bacterial growth rate*
gamb = 1;   %% killing rate*
k=10^(-2);  %% diffusion coefficient for the macrophages
chi = 1;    %% macrophage chemotaxis constant*
sigm = 1;   %% activation rate for macrophages*
gamm = 1;   %% deactivation rate for macrophages*

%% define simulation parameters

GridNum = 500;      %% number of nodes in the computational domain
Dt = 0.01;          %% time step
TotalTime = 10;     %% total simulationtime

x = linspace(-100,100,GridNum);
Dx = x(2) - x(1);

Skip = 1;
Steps = ceil(TotalTime./Dt./Skip);

D = Db.*Dt./Dx.^2;
L = k.*Dt./Dx.^2;
sigb = sigb.*Dt;
gamb = gamb.*Dt;

chi = chi.*Dt./4./Dx;
sigm = sigm.*Dt;
gamm = gamm.*Dt./2;

%% define initial conditions

b(:,1) = exp(-0.1.*x.^2);
m(:,1) = zeros(size(x));
Time(1) = 0;

%% define matrices

Vec = (1:GridNum);

BLeft =   sparse(Vec,Vec,1+D-sigb./2,GridNum,GridNum) ...
    + sparse(Vec,circshift(Vec,[0 -1]),-D./2,GridNum,GridNum) ...
    + sparse(Vec,circshift(Vec,[0 1]),-D./2,GridNum,GridNum);
```

```matlab
BRight =   sparse(Vec,Vec,1-D+sigb./2,GridNum,GridNum) ...
      + sparse(Vec,circshift(Vec,[0 -1]),D./2,GridNum,GridNum) ...
      + sparse(Vec,circshift(Vec,[0 1]),D./2,GridNum,GridNum);


%%%%%%%%%%%%%%%%%%%%%%%%%%%%%%%%%%%%%%%%%%%%%%%%%%%%
%%%%%%%%%%%%%%%%%%%%%%

%% Time Stepping

for n = 1:Steps

   b(:,n+1) = b(:,n);
   m(:,n+1) = m(:,n);

   for k = 1:Skip

      B2 = circshift(b(:,n+1),[0 -1]) - b(:,n+1);
      B3 = b(:,n+1) - circshift(b(:,n+1),[0 1]);

   MLeft =   sparse(Vec,Vec,1+chi.*(B2-B3)+gamm+L,GridNum,GridNum) ...
         + sparse(Vec,circshift(Vec,[0 -1]),chi.*B2+L,GridNum,GridNum) ...
         + sparse(Vec,circshift(Vec,[0 1]),-(chi.*B3-L),GridNum,GridNum);

   MRight =   sparse(Vec,Vec,1-L-chi.*(B2-B3)-gamm,GridNum,GridNum) ...
         + sparse(Vec,circshift(Vec,[0 -1]),-(chi.*B2-L./2),GridNum,GridNum) ...
         + sparse(Vec,circshift(Vec,[0 1]),chi.*B3+L./2,GridNum,GridNum);

   SourceB = BRight*b(:,n+1) - gamb.*m(:,n+1).*b(:,n+1);
   SourceM = MRight*m(:,n+1) + sigm.*b(:,n+1);

   b(:,n+1) = BLeft\SourceB;
   m(:,n+1) = MLeft\SourceM;
   B(n)=trapz(b(:,n+1));
   M(n)=trapz(m(:,n+1));
   t(n)=n*Dt  ;

   end

   [~,in]=max(sign(x').*b(:,n+1));
   xpeak(n)=x(in);
clf;
plot(x,b(:,n+1))
hold on
plot(x,m(:,n+1),'r')
plot(xpeak(n),b(in,n+1),'o')
mov(:,n) = getframe;

end
clf;
 figure
   plot(t,abs(xpeak))
```